# Power law shapes for leading-edge blunting with minimal standoff distance in low-density hypersonic flow

**W. F. N. Santos**

*Combustion and Propulsion Laboratory, National Institute for Space Research, Cachoeira Paulista, SP 12630-000 Brazil*

**Abstract.** The steady-state aerodynamic characteristics of power law shaped leading edges immersed in high-speed rarefied air flow are examined by using a Direct Simulation Monte Carlo method. The work is motivated by interest in investigating power-law shaped leading edges as possible candidates for blunting geometries of hypersonic configurations. The aerodynamic performance of power law shapes is compared to a corresponding round leading edge shape based on equivalent shock standoff distance. For the flow conditions considered, the analysis shows that round leading edges provide smaller stagnation point heating and smaller drag than power law shapes for equivalent shock standoff distance.

## 1 Introduction

Certain hypersonic configurations, such as waveriders, are designed analytically with infinitely sharp leading edges for shock wave attachment. The shock wave acts as a valve in order to prevent spillage of higher pressure airflow from the lower side of the vehicle to the upper side, resulting in a high-pressure differential and enhanced lift. As any practical waverider will have some degree of leading edge bluntness for heat transfer, manufacturing and handling concerns, the predicted performance of these configurations may not be achieved. Moreover, because of the viscous effects, the shock wave will be detached from the leading edge and, hence, the aerodynamic performance of the vehicle may be degraded from ideal performance.

Power law shapes ($y \propto x^n, 0 < n < 1$) may provide the required bluntness for heat transfer, manufacturing and handling concerns with reduced departures from ideal aerodynamic performance. This concept is based on the work of Mason and Lee [1], who have pointed out that, for certain exponents, power law shapes exhibit aerodynamic properties similar to geometrically sharp shapes. They suggested the possibility of a difference between shapes that are geometrically sharp and shapes that behave aerodynamically as if they were sharp. Mason and Lee [1] showed that power law shapes have an infinity body slope and yet have zero radius of curvature at the nose for certain values of power law exponent. Furthermore, their investigation predicts that the derivative of the pressure coefficient with respect to the body coordinates $dC_p/ds \to -\infty$ at $x = 0$, for $2/3 < n < 1$, a characteristic of a sharp body. This suggests that may be advantage to using a power law shape as a leading-edge blunting geometry, since zero radius of curvature at the nose will tend to lower shock standoff and drag, whereas infinite slope will tend to decrease the stagnation region heating.

The sensitivity of the pressure gradient and the stagnation point heating to shape variations of such leading edges has been investigated by Santos and Lewis [2] for the idealized situation of two-dimensional rarefied hypersonic flow at zero angle of incidence, and by Santos and Lewis [3] at positive angle of attack. Through the use of Direct Simulation Monte Carlo (DSMC) method, they showed that the pressure gradient behavior on the power law shapes in a rarefied environment is in agreement with that obtained by Mason and Lee [1] by employing Newtonian analysis.

The emphasis of this work is to compare power law leading edges with round leading edges in order to determine which geometry is better suited as a blunting profile in terms of shock standoff distance. Thus, for the same shock standoff distance, the stagnation point heating and the total drag will be the basis of comparison between these leading edges.

The simulation is concerned with the transitional flow regime, high altitude/kigh Knudsen number. At high altitude/kigh Knudsen number, the degree of molecular non-equilibrium is such that the Navier-Stokes equations are inappropriate. Therefore, DSMC method will be employed in order to calculate the rarefied hypersonic two-dimensional flow on the leading edge shapes.

## 2 Leading-edge geometry definition

The power-law shapes are modelled by assuming a sharp leading edge of half angle $\theta$ with a circular cylinder of radius $R$ inscribed tangent to this wedge. The power law shapes, given by $y = ax^n$, $0 < n < 1$, are also inscribed tangent to the wedge and the cylinder at the same common point where they have the same slope angle. The circular cylinder radius provides a reference for the amount of blunting desired on the leading edge. It was assumed a leading edge half angle of 10 deg, a circular cylinder diameter of $10^{-2}$m and power law exponents of $1/2, 0.6, 2/3, 0.7, 3/4$ and $0.8$.

From geometric considerations, the power law constant $a$ is obtained by matching slope on the wedge, circular cylinder and power law shapes at the tangency point. The common body height $H$ at the tangency point is equal to $2R\cos\theta$, and the body length $L$ from the nose to the tangency point in the axis of symmetry is given by $nH/2\tan\theta$.

The round leading edges are modelled by following the same procedure adopted for the power law leading edges. Figure 1 illustrates this construction for power law leading edge of $n = 1/2$ and a round leading edge with nose radius $R_N$ of $1.25 \times 10^{-3}$m.

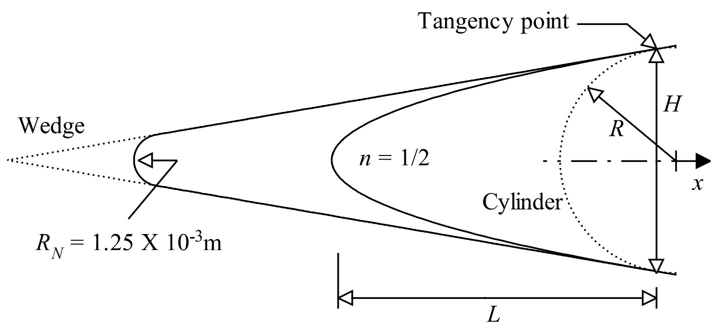


**Fig. 1.** Drawing illustrating the leading edge geometry

## 3 Computational method and procedure

DSMC method [4] is the most accurate and credible procedure for computing leading edge flow field and surface effects in the transitional flow regime. The DSMC method simulates real gas flows with various physical processes by means of a huge number of modelling particles, each of which is a typical representative of great number of real gas molecules, each one with a position, velocity and internal energy. The state of particles is stored and modified with time as the particles move, collide, and undergo boundary interactions in simulated physical space.

The molecular collisions are modelled using the variable hard sphere (VHS) molecular model [5]. In this model, the temperature dependence of the viscosity is considered by a variable cross section that is inversely proportional to the relative collision energy between the colliding molecules. Time is advanced in discrete steps such that each step is small in comparison with the mean collision time [4]. The simulation is always calculated as unsteady flow. However, a steady flow solution is obtained as the large time state of the simulation.

The energy exchange between kinetic and internal modes is controlled by the Larsen-Borgnakke statistical model [6]. Simulations are performed using a non-reacting gas model consisting of two chemical species, $N_2$ and $O_2$. Energy exchanges between the translational and internal modes are considered. The relaxation numbers of 5 and 50 were used for the rotation and vibration, respectively.

The flow field is divided into a number of regions, which are subdivided into computational cells, and the cells are further subdivided into subcells. The cell provides a convenient reference for the sampling of the macroscopic gas properties, and the subcell for the selection of the collision partners. The dimensions of the cells must be such that the change in flow properties across each cell is small. The linear dimensions of the cells should be of the order of the local mean free path or even smaller [4].

Numerical accuracy in DSMC method depends on the grid resolution chosen as well as the number of particles per computational cell. Both effects were investigated in order to determine the number of cells and the number of particles required to achieve grid independence solutions. A discussion of both effects on the surface quantities is described in Santos and Lewis [7] for round leading edges, and in Santos [8] for power law shapes.

The flow conditions used in the present simulation are those given by Santos and Lewis [2] and summarized in Table 1. The freestream velocity $V_\infty$ is assumed to be constant at 3.5 km/s, which corresponds to freestream Mach number $M_\infty$ of 12. The wall temperature $T_w$ is assumed constant at 880 K. Diffuse reflection with complete thermal accommodation is the condition applied to the body surface. The freestream Knudsen number, defined as the ratio of the molecular mean free path in the gas to a characteristic dimension of the flow field, $Kn_\infty = \lambda_\infty/D$ corresponds to 0.0903, where the circular cylinder diameter $D$ was used as the characteristic dimension. Finally, the freestream Reynolds number by unit meter $Re_\infty$ is 21455.

**Table 1.** Freestream conditions

| $T_\infty$(K) | $p_\infty$(N/m$^2$) | $\rho_\infty$(kg/m$^3$) | $\mu_\infty$(Ns/m$^2$) | $n_\infty$(m$^{-3}$) | $\lambda_\infty$(m) |
|---|---|---|---|---|---|
| 220.0 | 5.582 | $8.753 \times 10^{-2}$ | $1.455 \times 10^{-2}$ | $1.8209 \times 10^{21}$ | $9.03 \times 10^{-4}$ |

## 4 Computational results and discussions

The purpose of this section is to compare and to discuss differences in the shock standoff distance, stagnation point heat transfer, and total drag coefficient due to changes in the leading edge shape. Two method of comparing power law shapes to round leading edges will be investigated: (1) power law shapes are compared to the corresponding round leading edge (circular cylinder), which generates the power law shapes, and (2) the equivalent round leading edge, which is generated from the computational results for the power law shapes. The equivalent round leading edge will yield the same shock standoff distance as the computed solutions (DSMC) presented for power law shapes. Thus, for the same shock standoff distance, the stagnation point heating and the total drag will be the basis of comparison between these leading edges.

The heat transfer coefficient at the stagnation point $C_{ho}$, the total drag coefficient $C_d$ and the dimensionless shock standoff distance $\delta/\lambda_\infty$ are illustrated in Fig. 2(a) as a function of the power law exponent $n$. For comparison purpose, $C_{ho}$, $C_d$, and $\delta/\lambda_\infty$ for the reference cylinder are 0.366, 1.520 and 1.646, respectively.

Compared to power law shapes, the reference cylinder provides low value to $C_{ho}$. Nevertheless, the reference cylinder presents high value to $C_d$, where the major contribution is given by the pressure drag coefficient (not shown). As expected, $\delta/\lambda_\infty$ for the reference cylinder is also larger than those for power law shapes. In comparison, $\delta/\lambda_\infty$ is 2.4 times larger than that for the $n = 1/2$ case, and it is one order of magnitude greater for the $n = 0.8$ case.

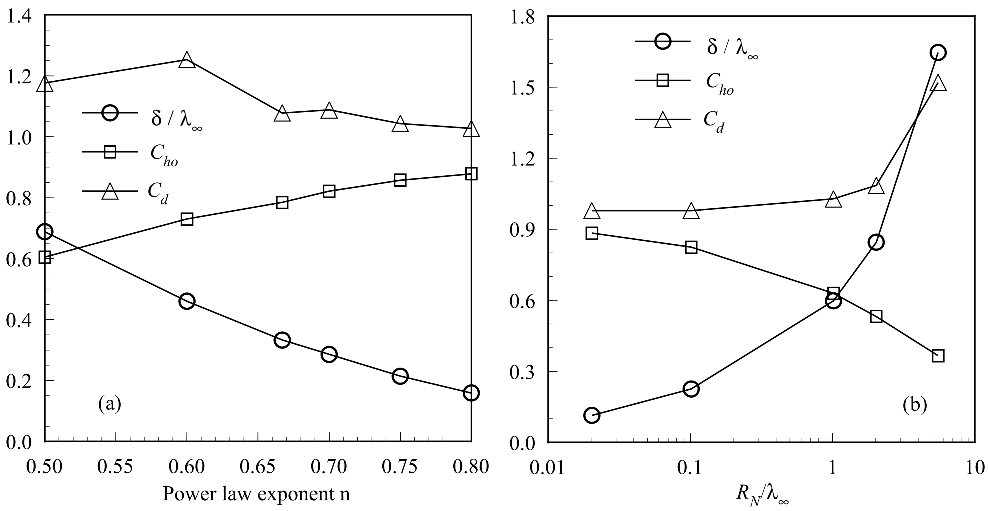


**Fig. 2.** Stagnation point heat transfer $C_{ho}$, total drag coefficient $C_d$, and shock standoff distance $\delta/\lambda_\infty$ for (**a**) power law leading edges, and (**b**) for round leading edges

These curves indicate that power law shapes perform better then the reference cylinder in terms of total drag coefficient and shock standoff distance. Nevertheless, the reference cylinder presents low stagnation heat transfer coefficient than power law shapes.

DSMC simulations were also performed for four round leading edges, besides the reference cylinder, with nose radii $R_N/\lambda_\infty$ of 0.02, 0.1, 1.0, and 2.0. The dependence of $C_{ho}$, $C_d$ and $\delta/\lambda_\infty$ on the nose radius $R_N$ is illustrated in Fig. 2(b). According to this figure, the stagnation heat transfer coefficient decreases with increasing the nose radius. This behavior seems to be in agreement with the continuum predictions for blunt body in that the heat flux scales inversely with the square root of the nose radius. Also, the total drag coefficient decreases with decreasing the nose radius, and approaches the value of 0.980 found for a wedge, as would be expected. A similar behavior is observed to the shock standoff distance in that it decreases with decreasing the nose radius. This is an expected behavior since the shock standoff distance scales with the nose radius for circular cylinder.

A second means of comparison between power law shapes and round leading edge is defined as equivalent round leading edge. The comparison is made between the shock standoff distance on the power law shapes and the round leading edge with an equivalent nose radius $R_{eq}$ that gives the same shock standoff distance found for power law shapes.

By using $\delta/\lambda_\infty$ for each one of the power law shapes from Fig. 2(a) as input, the equivalent nose radius $R_{eq}/\lambda_\infty$ is obtained from Fig. 2(b). As a result, one obtains $R_{eq}/\lambda_\infty$ of 1.388, 0.678, 0.365, 0.249, 0.093 and 0.053, which correspond to power law exponents of 1/2, 0.6, 2/3, 0.7 and 0.8, respectively.

The comparison of the stagnation heat transfer coefficient and total drag coefficient for power law shapes and for round leading edges that correspond to the equivalent nose radii that match power law body shock wave standoff distance is displayed in Fig. 3. Referring to Fig. 3, it is seen that power law shapes provide larger drag coefficient and larger stagnation heat transfer than those round leading edges defined by the equivalent nose radius. As a result, power law shapes may not be the ideal leading edge blunting geometry.

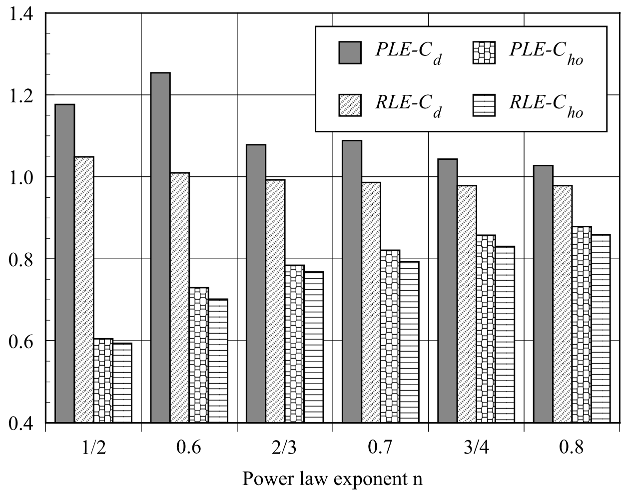


**Fig. 3.** Stagnation heat transfer coefficient $C_{ho}$ and total drag coefficient $C_d$ that correspond to the equivalent round leading edges with comparable shock standoff distance to power law shapes. PLE and RLE mean power-law leading edge and round leading edge, respectively

This conclusion is further strengthened by comparing, for instance, the power law shape given by $n = 1/2$ with the equivalent shock standoff distance for the round leading edge, and the original reference cylinder. Figure 1 displays this comparison where the reference cylinder radius is $R_N/\lambda_\infty = 5.5$, the radius for the equivalent round leading edge is $R_{eq}/\lambda_\infty = 1.388$ and the radius of curvature for the $n = 1/2$ case is $R_c/\lambda_\infty = 0.961$. It is worthwhile to mention that one-half power law geometry is the only power law geometry with a finite radius of curvature at the leading edge. It is given by $R_c = a^2/2$, where $a$ is the power law constant. Referring to Fig. 1, it is seen that the equivalent round leading edge ($R_N = 1.25\times10^{-3}$m corresponds to $R_{eq}/\lambda_\infty = 1.388$) for shock standoff distance has not only smaller drag and stagnation heat transfer coefficient but it also has more volume than the power law geometry. In this context, for actively cooled leading edges, large portion of coolant may be placed within the leading edge for heat absorption.

## 5 Concluding remarks

The computations of a rarefied hypersonic flow on power law leading edges have been performed by using the DSMC method. The calculations provided information concerning the nature of the aerodynamic quantities at the vicinity of the nose resulting from variations in the body shape. The emphasis of the investigation was to compare power law shapes with round leading edges in order to determine which geometry is better suited as a blunting profiles in terms of shock standoff distance. Equivalent round leading edges were defined with the same shock standoff distance yielded by power law shapes. With the same shock standoff distance, round leading edges were shown to produce much smaller total drag and smaller stagnation heat transfer. Hence, if heating and drag are considered the primary issues in leading-edge design, then round leading edges are superior to power law leading edges.

## References


1. W. H. Mason, J. Lee: J. of Spacecraft and Rockets **31**, 378 (1994)
2. W. F. N. Santos, M. J. Lewis: J. of Spacecraft and Rockets **39**, 917 (2002)
3. W. F. N. Santos, M. J. Lewis: 'Angle of Attack Effect on Rarefied Hypersonic Flow over Power Law Shaped Leading Edges'. In: *23rd International Symposium on Rarefied Gas Dynamics, Whistler, BC, Canada, July 20–25, 2002*
4. G. A. Bird: *Molecular Gas Dynamics and the Direct Simulation of Gas Flows*, 2nd edn. (Oxford University Press, Oxford, England, UK, 1994)
5. G. A. Bird: 'Monte Carlo Simulation in an Engineering Context'. In: *Progress in Astronautics and Aeronautics: Rarefied Gas Dynamics*, ed. by Sam S. Fisher (AIAA, New York 1988) vol. 74, pp.239–255
6. C. Borgnakke, P. S. Larsen: J. of Computational Physics **18**, 405 (1975)
7. W. F. N. Santos, M. J. Lewis: 'Aerodynamic Heating Performance of Power Law Leading Edges in Rarefied Hypersonic Flow'. In: *36th AIAA Thermophysics Conference, AIAA paper 2003-3894, Orlando, FL, June 23–26, 2003*
8. W. F. N. Santos: 'Direct Simulation Monte Carlo of Rarefied Hypersonic Flow on Power Law Shaped Leading Edges'. PhD Thesis, University of Maryland, College Park, MD, (2001)
9. W. F. N. Santos: 'Shock Wave Shapes on Power Law Leading Edges'. In: *24th International Symposium on Shock Waves, Beijing, China, July 11–16, 2004*